Molecular Dynamics Simulation Study of Water Adsorption on Hydroxylated Graphite Surfaces

Sylvain Picaud,* B. Collignon, and Paul N. M. Hoang

Laboratoire de Physique Moléculaire—UMR CNRS 6624, Faculté des Sciences, La Bouloie, Université de Franche-Comté, F-25030 Besançon Cedex, France

J. C. Rayez

Laboratoire de Physico-Chimie Moléculaire—UMR CNRS 5803, Université de Bordeaux I, 351 cours de la Libération, F-33405 Talence Cedex, France

Received: November 28, 2005; In Final Form: February 20, 2006

In this paper, we present results from molecular dynamic simulations devoted to the characterization of the interaction between water molecules and hydroxylated graphite surfaces considered as models for surfaces of soot emitted by aircraft. The hydroxylated graphite surfaces are modeled by anchoring several OH groups on an infinite graphite plane. The molecular dynamics simulations are based on a classical potential issued from quantum chemical calculations. They are performed at three temperatures (100, 200, and 250 K) to provide a view of the structure and dynamics of water clusters on the model soot surface. These simulations show that the water−OH sites interaction is quite weak compared to the water−water interaction. This leads to the clustering of the water molecules above the surface, and the corresponding water aggregate can only be trapped by the OH sites when the temperature is sufficiently low, or when the density of OH sites is sufficiently high.

1. Introduction

Transmission electron microscopy (TEM) studies have shown that soot emitted by aircraft are made of nanocrystallites containing graphite-type layers arranged in an onionlike structure forming quasispherical particles with diameters in the 20−50-nm range.[1] Results of recent Raman spectroscopy revealed that these graphite layers are partially oxidized and that they contain a certain number of hydrophilic sites such as carbonyl, carboxyl, phenol, and hydroxyl groups.[2] The presence of such polar groups can affect the adsorption of polar species such as water, and soot can acquire a substantial amount of water as shown by thermodynamics measurements of the corresponding adsorption isotherms.[3]

This affinity of soot particles for water attracts some attention because of its implication in the nucleation of ice particles in aircraft contrails.[4,5] Indeed, the condensation of water molecules around soot particles results in the formation of artificial cirrus that may impact the chemistry of the upper troposphere/lower stratosphere.[6]

Despite the likely importance of atmospheric soot particles, few studies on this topic have been reported so far, and a detailed theoretical understanding of the water nucleation dynamics on soot remains challenging. So, for example, the semiempirical PM3 method has been used to characterize the equilibrium configuration of up to three water molecules with partially oxidized graphite surfaces.[7−9] It has been thus shown that vacancies and/or OH and COOH hydrophilic groups can favor the formation of small water aggregates on the graphite surface. Adsorption equilibrium of a much larger number of water molecules has also been studied on a partially oxidized graphite surface by means of grand canonical Monte Carlo (GCMC) simulations[10−12] based on a classical description of the interaction potentials between water and the graphite surface. These works have shown that the water adsorption is strongly dependent on the presence and on the arrangement of the hydrophilic groups. GCMC simulations have also been used to calculate adsorption isotherms of water on activated carbon adsorbents modeled by polar oxygen-containing sites (hydroxyl, carboxyl, and carbonyl) placed on the walls of carbon slit pores.[13] The corresponding results show that adsorption at low pressure is dictated by the local distribution of hydrophilic sites and that the amount of water adsorbed in the pores is mainly affected by the number of oxygen atoms on the surface, rather than by their functionality.[13]

Although these previous theoretical works have taken into account the influence of hydrophilic groups on water adsorption on graphite surfaces, they were based on simple classical potentials issued from the literature and, for example, no local modification such as structure or charge distribution of the graphite surface upon oxidation was taken into account. Moreover, these works were based on interaction potential optimization or Monte Carlo simulations, and thus, information on neither the temperature influence nor the dynamics of the water adsorption was obtained.

In previous papers, we combined quantum chemical calculations and molecular dynamics (MD) simulations to study the adsorption of water molecules on a graphite surface containing carboxyl (COOH) groups.[14,15] The quantum calculations were used to calculate the geometry of the COOH group anchored on the graphite surface and to derive a pair potential for the water−COOH site interaction that was then used in the classical

* Electronic address: sylvain.picaud@univ-fcomte.fr. Phone number: +33381666478. Fax: +33381666475.

10.1021/jp056889t CCC: $33.50
Published on Web 04/06/2006

MD simulations. These simulations showed that such a partially oxidized graphite surface is characterized by a high affinity for water molecules. Indeed, at low water coverage, the COOH group acts as a strong trapping site for the water molecules, that then becomes a nucleation center for other water molecules at higher coverage, leading to the formation of large aggregates attached to the COOH site. In a subsequent study, we used quantum calculations to compare the first steps of water adsorption on COOH and OH sites anchored on both the face and the edge of a graphite nanocrystallite.[16,17] This quantum study showed that the sites anchored on the edge of the nanocrystallite are more attractive for water than the sites anchored on its face and that the water adsorption energy value on COOH is twice the value calculated on a OH site, indicating a preferential adsorption of water on graphite surfaces containing COOH rather than OH sites.

In the present paper, we investigate the influence of a partially oxidized graphite surface on water adsorption, by focusing on OH sites. We make use of MD simulations to characterize the structure and the dynamics of water molecules adsorbed on a hydroxylated graphite surface, for various water coverages. The hydroxylated surface was built from several OH sites randomly anchored on a planar graphitic layer, and the pair potential used in the simulations is based on a charge distribution supplied by ab initio calculations. The MD simulations are performed at 100, 200, and 250 K (i.e., a very low temperature and higher temperatures typical of the boundaries of the stratospheric temperature range), to quantify the temperature effects on the water adsorption characteristics.

2. Details of the Molecular Dynamics Simulations

The MD simulations have been carried out by standard methods[18] in a similar way to the previous study of water adsorption on a graphite surface containing anchored COOH groups.[15] The graphite substrate is represented by three fixed layers of C atoms which occupy the bottom of the simulation box. The two innermost layers have the pure graphite geometry, whereas the surface layer contains a random distribution of OH sites, between 1 and 15 sites. The geometry of these OH sites is issued from ab initio calculations based on the two-layer ONIOM method.[16,17] Note that a reflecting ceiling located at 30 Å above the graphite surface has been added in the simulation box, to prevent water molecules from escaping. No periodic conditions were imposed along the *z* direction perpendicular to the graphite plane. Water adsorption can occur thus on one side of the graphite system, only.

In the previous quantum calculations,[16,17] the geometry of only one OH group anchored on a large cluster containing 80 C atoms + 22 H atoms (used to saturate the edges of the cluster) was optimized, leading to a structure where the 16 C atoms nearest to the OH anchoring position have been mostly relaxed along the *z* direction perpendicular to the graphite surface. Here, in the MD simulations, we model the hydroxylated graphite surface by randomly scattering several OH sites, with the criterion that two sites must not overlap.[15] Note that each OH site contains the OH group, the extra H atom (see refs 16 and 17), and the relaxed 16 nearest C atoms (Figure 1).

The (x, y) size of the simulation box is equal to $x = 46.86$ Å and $y = 46.74$ Å, along the directions parallel to the graphite surface. This corresponds to a surface equal to 2190 Å^2, that is consistent with the size of the planar nanocrystallites arranged in the onionlike structure observed in soot particles.[3] Indeed, spherical soot particles are typically characterized by diameters in the 20−50-nm range,[1] corresponding to an outer surface exposed to water molecule adsorption between 125 000 and 785 000 Å^2. These values would correspond to between 57 and 358 nanocrystallites similar in size to our simulation box. Various coverages up to 128 moving water molecules have been considered in the simulations.

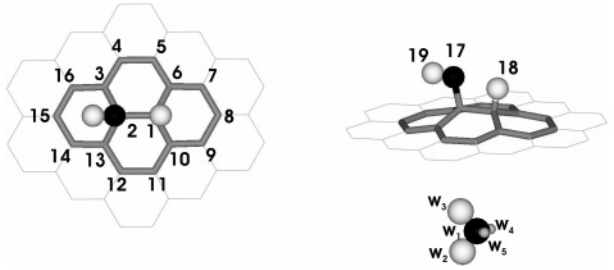

Figure 1. Top and side views of one OH site anchored on a graphite surface. Such a site contains the OH group, the extra H atom (see text), and the relaxed 16 nearest C atoms. The black and white circles represent the oxygen and hydrogen atoms, respectively, whereas the carbon atoms are represented by gray sticks (large sticks for the relaxed atoms and thin sticks for the rest of the graphite surface). The water molecule as described by the TIP5P model is also shown (O and H atoms are represented by black and white circles, respectively, whereas the small gray circles correspond to the positions of the two negative charges of the TIP5P model). The numbers on the atoms correspond to the numbering used in Table 2 for the calculation of the charges issued from the ab initio calculations.

TABLE 1: Lennard−Jones Parameters Used in the Present MD Simulations for the Calculations of the Dispersion−Repulsion Interactions between TIP5P Water and the Hydroxylated Graphite Surface

interacting pair	σ (Å)	ϵ (kJ/mol)
C−O$_w$	3.275	0.388
O−O$_w$	3.431	0.670
H−O$_w$	0.000	0.000
O$_w$−O$_w$	3.120	0.669

The translational equations of motion are solved by using the Verlet algorithm, and a predictor−corrector method based on the quaternion representation of the molecular orientations is used for the orientational equations of motion, with a time step of 2.2 fs.[18] Long runs are performed, involving 250 000 time steps (i.e., 550 ps) for equilibrating the system, followed by 200 000 additional time steps (440 ps) for collecting the data. The initial positions of the water molecules are randomly scattered above the hydroxylated graphite surface. The initial velocities for each moving molecule are taken from a Boltzmann distribution corresponding to the desired simulation temperature. At the beginning of the simulation, i.e., during the first 25% of the equilibration period, the temperature is slowly increased up to the desired temperature. During the production run, the temperature is held constant by using a Berendsen thermostat in the NVT ensemble. The simulations are performed at 200 and 250 K, temperatures which are typical of the boundaries of the temperature range in the troposphere, and also at a much lower temperature (100 K) for comparison of the temperature effects on the dynamics of the water molecules.

The interaction potential for the adsorbate−substrate system (V_{ws}) is written as the sum of the water molecules−carbon atoms interaction (V_{wc}) and the water molecules−active group (H+OH) interaction (V_{wd}). These potentials V_{wc} and V_{wd} are the sum of pairwise atom−atom Lennard−Jones and charge−charge interactions. The Lennard−Jones parameters (Table 1) are issued from the literature. They are based on potentials developed for the interaction between water molecules and activated carbon pores[19] and for the interaction between methanol and water molecules.[20]

TABLE 2: Values of the Charges Used to Calculate the Electrostatic Interactions between Water Molecules and the Hydroxylated Graphite Surface in the MD Simulations[a]

atom	number	q (e)
C	(1)	0.250
C	(2)	0.400
C	(3)	−0.222
C	(4)	0.060
C	(5)	0.000
C	(6)	−0.133
C	(7)	0.020
C	(8)	−0.030
C	(9)	0.020
C	(10)	−0.133
C	(11)	0.000
C	(12)	0.060
C	(13)	−0.222
C	(14)	0.118
C	(15)	−0.115
C	(16)	0.118
O	(17)	−0.650
H	(18)	0.079
H	(19)	0.380
O_w	(w1)	0.000
H_w	(w2)	0.241
H_w	(w3)	0.241
site$_w$	(w4)	−0.241
site$_w$	(w5)	−0.241

[a] The values of the charges located on the OH active site and the surrounding C atoms are issued from ab initio calculations (see text). Note that there is no charge for the C atoms located far from an active group. The charges on the water molecules are issued from the TIP5P model (ref 23). The numbering of the atoms is indicated in Figure 1.

To obtain the electrostatic potential between the water molecules and the hydroxylated graphite, we have determined a set of charges on the surface as follows. First, one H+OH group has been anchored at the center of a large $C_{80}H_{22}$ cluster, and the charges of the atomic sites of this cluster have been calculated at an ab initio level by fitting the electrostatic potential around the cluster using the Merz−Singh−Kollman (MSK) scheme.[21,22] Within this scheme, charges are almost negligible except for those around the OH position (i.e., the H+OH group and the 16 nearest C atoms). Similar calculations have then been performed when adsorbing up to 4 water molecules around the OH group, to quantify possible charge transfer upon water adsorption. The results show that the values of the calculated charges differ slightly from one situation to another, but no significant charge transfer has been obtained between the adsorbate and the hydroxylated $C_{80}H_{22}$ cluster. On the basis of these conclusions, we choose the charges calculated without water for the potential used in the simulations. These charges are given in Table 2. Then, when building up the hydroxylated graphite surface by scattering nonoverlapping OH sites, we have assumed that the charge redistribution around a site is not modified by the presence of surrounding OH groups.

To describe the interaction V_{ww} between the water molecules, we have used the TIP5P model[23] that involves five sites: two sites bearing positive charges (+0.241 e) located on the two hydrogen atoms and two sites bearing charges of equal magnitude and opposite sign (−0.241 e) placed on the lone-pair interaction sites; the fifth site is located on the oxygen to characterize the dispersion−repulsion interaction. Note that we have also performed preliminary calculations with the TIP4P potential that involves only four sites on water.[24] However, the structures and energies of small water aggregates (up to five molecules) optimized using this classical potential where less comparable with results based on the ab initio ONIOM method than those found when using the TIP5P potential (see below). Thus, we decided to perform the MD simulations using the TIP5P model only.

TABLE 3: Average Energy per Molecule (in kJ/mol) for Different Water Coverages when There Is Only One OH Site on the Graphite Surface[a]

no. water molecules	V_{ws}	V_{ww}	V_{total}	$V_{abinitio}$
1	−22.5	0.0	−22.5	−16.7
2	−13.7	−13.8	−27.5	−24.8
3	−11.8	−17.2	−29.0	−30.4
4	−10.7	−21.1	−31.8	−30.5
5	−8.6	−30.3	−38.9	−32.2
8	−7.7	−33.2	−40.9	
12	−6.4	−34.3	−40.7	
13	−4.4	−35.7	−40.1	

[a] For aggregates with up to five molecules, the results are issued from an optimization procedure at 0 K. For the larger aggregates, the results come from MD simulations at 100 K. Values from the ab initio calculations of ref 16 are also indicated for comparison.

Because we use the TIP5P model for water,[23] that has been originally derived without any long-range corrections, the lateral interactions between water molecules have been calculated in the present simulations with a spherical cutoff method rather than using the more sophisticated Ewald summation. Note that the use of such cutoff methods to account for long-range electrostatic interactions can lead to questionable results especially when calculating integrated quantities with too short cutoff values.[25] Thus, it has been shown that some properties of liquid water calculated with the TIP5P potential can differ when considering different ways of handling long-range corrections.[26] Therefore, to check the convergence of the results, different cutoff values have been considered in our simulations, ranging from 9.0 Å (corresponding to the cutoff originally used by Mahoney and Jorgensen[23]) to a very large cutoff of 23.0 Å (corresponding to approximately half the MD box). Slight differences have been evidenced in our simulations when comparing results obtained with short (9.0 Å) and larger (15.0 Å) cutoffs, although the conclusions are qualitatively the same. By contrast, simulations performed with a very large cutoff of 23.0 Å give results quantitatively comparable to those obtained from simulations performed with a cutoff of 15.0 Å, showing the convergence of the calculations. As a consequence, because similar results and conclusions are obtained when using large cutoff values, only the results obtained with the largest cutoff value (23.0 Å) are given in the present paper. Note that the convergence of the conclusions obtained with different large cutoff values indicates that our results would not strongly depend on the way of calculating the long-range electrostatic interactions. The water molecules are treated as rigid bodies. The polarization effects between the adsorbate and the substrate have been disregarded, and all the interactions are calculated in the direct space.

3. Results of the Simulations

3.1. Classical Potential Accuracy. To check the accuracy of the potential used in our simulations, we have performed an energy optimization of small water aggregates (up to five molecules) on a graphite surface containing one OH site and compared the corresponding equilibrium structures and energy values with those issued from our previous ab initio study.[17]

The results of the energy optimization show that both the geometry of the equilibrium configurations (not shown) and the corresponding energy values (Table 3) are similar to that obtained with the ab initio method. When the number n of

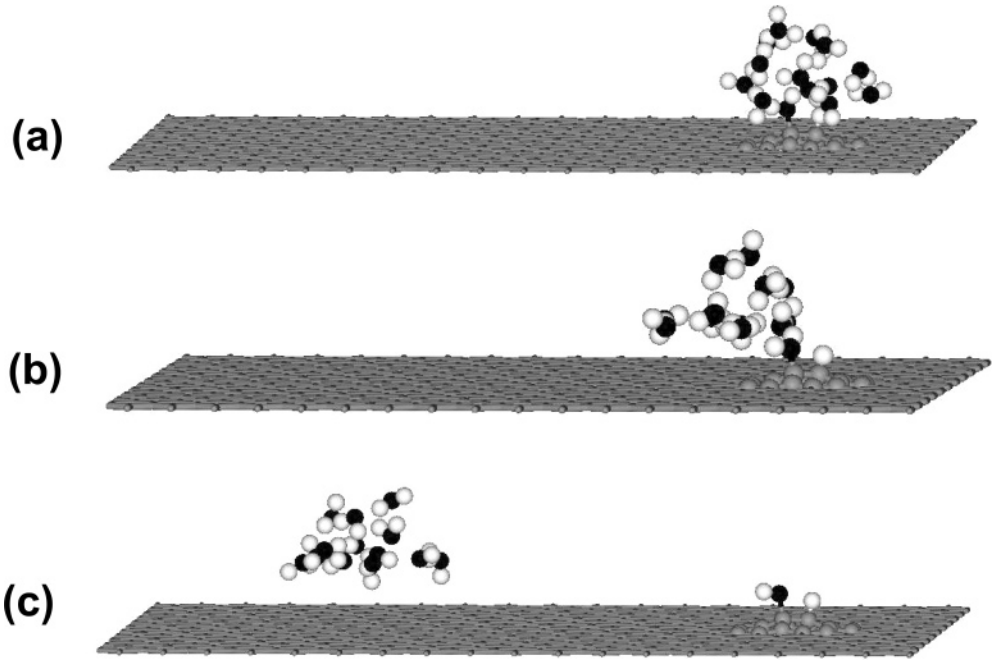

Figure 2. Snapshots issued from the simulations at (a) 100, (b) 200, and (c) 250 K for a small aggregate (13 water molecules) adsorbed on a hydroxylated graphite surface containing only one OH site. Only the surface layer of the hydroxylated graphite is shown for clarity. The oxygen and hydrogen atoms are represented by black and white circles, respectively. The C atoms around the OH site are represented by gray circles, whereas the other C atoms of the surface are represented by gray sticks.

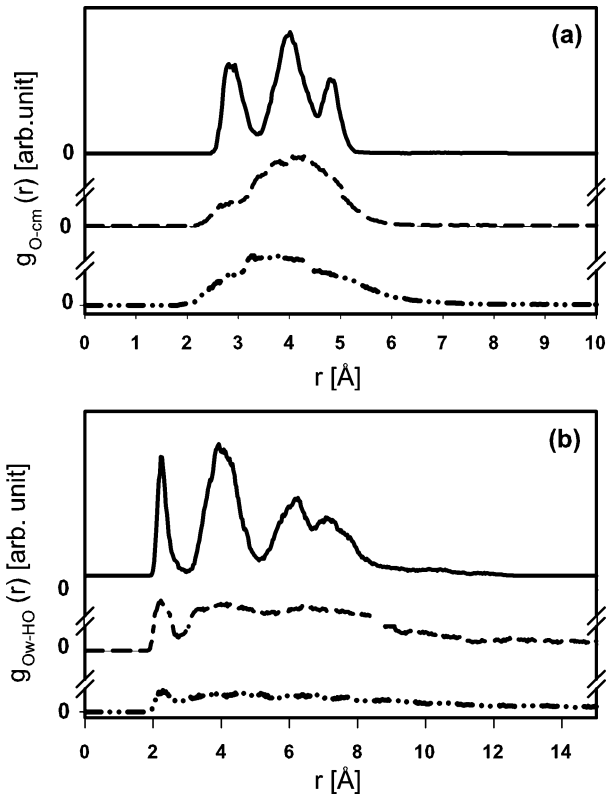

Figure 3. (a) Pair radial distribution functions $g_{O-cm}(r)$ of the distance between an O atom pertaining to a water molecule and the center of mass of the water aggregate and (b) pair distribution functions $g_{Ow-HO}(r)$ of the distance between an O atom pertaining to the water molecule and the H atom of the OH site, issued from molecular dynamics simulations at 100 (full curve), 200(broken curve), and 250 K (dashed−dotted curve), for a small water aggregate (13 water molecules) adsorbed on a hydroxylated graphite surface containing only one OH site.

molecules increases from 1 to 4, the adsorption energy ranges from −22.5 to −31.8 kJ/mol, and the main contribution to this potential energy comes from the electrostatic interactions. Note that the carbon atoms substantially contribute to the total interaction. For example, when $n = 1$, the interaction between water and carbon atoms is equal to $V_{wc} = -13.6$ kJ/mol, whereas the interaction coming from the H+OH site accounts for −8.9 kJ/mol.

This large contribution of the C atoms can partly explain the difference between classical and quantum calculations. Indeed, the $C_{80}H_{22}$ cluster used in the quantum chemical calculations represents only a small area of the graphite system considered in the present simulations. Moreover, the quantum calculations probably underestimate the contribution V_{wc} because it mainly comes from the dispersion−repulsion interactions that are not fully included in the ONIOM method used previously.[17]

In the present simulations, the charge distribution on the water molecules is represented by the TIP5P potential because it is well suited for lateral interactions between water molecules.[23] This charge distribution is, however, quite different from the one issued from the MKS calculations, and this can lead to differences in the electrostatic interaction between the water molecules and the graphite surface. However, these differences are smoothed out when the number of water molecules increases and both quantum and classical energy values agree quite well (up to 4 water molecules), because of the increasing influence of the lateral interactions between water molecules.

On the basis of these results (equilibrium geometry + potential energy), we can reasonably conclude that our classical potential is accurate enough to model the water-activated graphite interaction, especially when considering large water coverage.

3.2. Simulations with One Active Site on the Graphite Surface. Let us detail now the results obtained with only one OH site implemented on the graphite surface for different water coverages.

We have first performed molecular dynamics simulations at 100, 200, and 250 K for an intermediate coverage of 13 molecules, a number that corresponds in fact to the number of molecules involved in three close packed hexagons in one layer

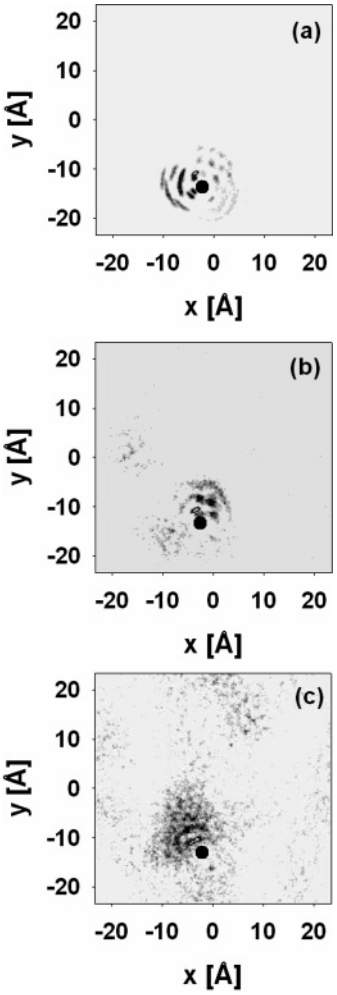

Figure 4. Distribution functions of the positions of oxygen atoms (of water molecules) projected in the (*x*, *y*) plane of the surface, for an aggregate containing 13 water molecules at (a) 100, (b) 200, and (c) 250 K, above a surface containing one OH site located at the center of the black circle.

of hexagonal ice.[27] For this number of molecules, the results of MD simulations show that the influence of the active group is not very sensitive from an energetic point of view and that the interactions are dominated by the large water−water contributions (Table 3) that lead to the formation of a water aggregate on the surface during the equilibration phase of the simulation, as confirmed by snapshots issued from the simulations (Figure 2).

To better characterize this water aggregate, we have calculated, then, pair radial distribution functions. For example, Figure 3a represents the distributions $g_{O-cm}(r)$ of the distances between the oxygen atoms of the water molecules and the center of mass of the water aggregate. This function indicates that the spatial extension of the water molecules around the center of mass of the 13 molecules is limited to about 4 Å at 100 K, 4.5 Å at 200 K, and 5 Å at 250 K and, thus, evidences that water molecules form a stable aggregate during the whole duration of the simulations.

The geometry of this water aggregate above the surface is mainly driven by the formation of hydrogen bonds between water molecules themselves and also between these water molecules and the OH site located on the hydroxylated surface. Such H-bonds can be characterized in the simulations through the calculations of some pair distribution functions $g_{XY}(r)$ that reflect the probability of finding a distance *r* between an X atom

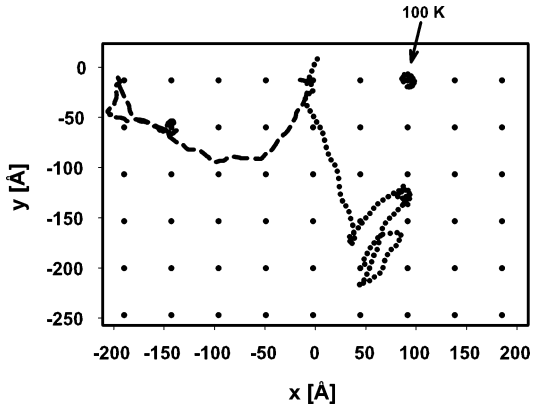

Figure 5. Trajectories in the (*x*, *y*) plane of the surface, of the center of mass of an aggregate containing 13 water molecules at 100 (full curve), 200 (broken curve), and 250 K (dotted curve), above a surface containing one OH site. Note that, during the simulations at 200 and 250 K, the mobility of the water aggregate is sufficiently large to move over the whole MD box. Then, in the present figure, we have chosen to draw the trajectory without putting it back in the MD box (due to periodic conditions), for clarity. As a consequence, the figure contains a periodic juxtaposition of equivalent boxes and then exhibits several OH sites (1 site per MD box). However, in the simulations, when the trajectory leaves the MD box from one side, its symmetric image enters the box from the other side, because of periodic conditions (see text).

TABLE 4: Average Energy per Molecule (in kJ/mol) for Different Water Coverages and Different Numbers of OH Sites on the Graphite Surface Issued from Molecular Dynamics Simulations at 100, 200, and 250 K[a]

temp	no. OH sites	no. water molecules	V_{ws}	V_{ww}	V_{total}
100 K	3 (set 1)	13	−4.2	−37.3	−41.5
		39	−4.6	−38.5	−43.1
		48	−3.0	−42.2	−45.2
		128	−2.2	−43.0	−45.2
	3 (set 2)	13	−5.1	−36.3	−41.4
		39	−5.7	−35.8	−41.5
		48	−4.5	−40.0	−44.5
		128	−2.7	−43.0	−45.7
	9	128	−2.7	−43.3	−46.0
	15	13	−7.8	−35.0	−42.8
	15	128	−3.9	−41.3	−45.2
200 K	3 (set 1)	13	−4.7	−32.5	−37.2
		39	−3.8	−37.5	−41.3
		48	−2.9	−38.8	−41.7
		128	−2.7	−40.9	−43.6
	3 (set 2)	13	−4.5	−32.7	−37.2
		39	−3.9	−37.0	−40.9
		48	−3.9	−37.8	−41.7
		128	−2.8	−40.9	−43.7
	9	128	−2.8	−41.0	−43.8
	15	13	−7.7	−32.7	−40.4
	15	128	−3.7	−40.3	−44.0
250 K	3 (set 1)	13	−4.9	−27.7	−32.6
		39	−3.5	−33.1	−36.6
		48	−3.6	−33.8	−37.4
		128	−2.4	−37.1	−39.5
	3 (set 2)	13	−5.1	−28.2	−33.3
		39	−3.5	−33.3	−36.8
		48	−3.3	−33.9	−37.2
		128	−2.6	−36.9	−39.5
	9	128	−2.8	−36.9	−39.7
	15	13	−6.8	−28.2	−35.0
	15	128	−3.3	−36.6	−39.9

[a] Set 1 and set 2 correspond to configurations in which the OH sites are far or close from each other, respectively (see text and Figures 6 and 7).

of the water molecules and an Y atom pertaining to the OH site. Note that, in our classical simulations, we can define H-bonds on a geometrical criterion only and we will consider

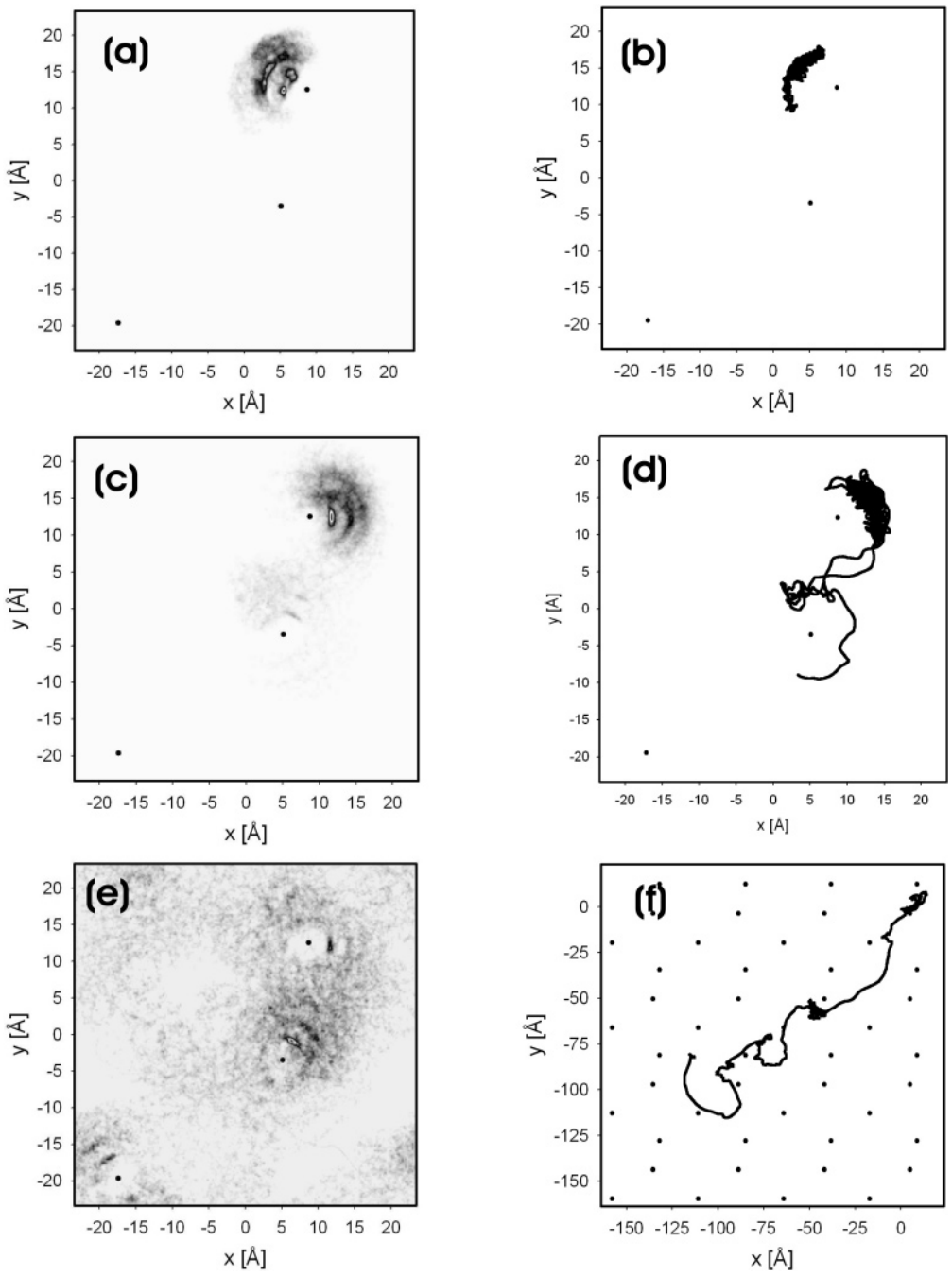

Figure 6. Distribution functions $h(x, y)$ of the positions of the oxygen atoms (of water molecules) projected in the (x, y) plane of the surface and trajectories of the aggregate center of mass for an aggregate containing 13 water molecules at 100 (a and b, respectively), 200 (c and d), and 250 K (e and f), above a surface containing three OH sites (black circles, set 1). Note that in part f periodic images of the simulation box are also represented.

that a possible H-bond is formed when the O−H distance is less than 2.5 Å, i.e., when a peak in the corresponding distribution function is evidenced between 1.5 and 2.5 Å. In the present calculations, such a peak appears clearly only in the pair distribution functions $g_{Ow-HO}(r)$ of the distance between an O atom pertaining to the water molecule and the H atom of the OH site at 100 K (see Figure 3b). This peak corresponds to the binding between a water molecule of the aggregate and the OH site, through an acceptor H-bond. At 200 K, a small peak is also evidenced around 2 Å, indicating that a H-bonding is also present at this temperature, but it is less pronounced than at 100 K. At 250 K, the H-bonding is much less probable, as indicated by the very small peak evidenced at 2.2 Å in the $g_{Ow-HO}(r)$ distribution function.

Another way to characterize the geometry of the water molecules during the simulations is the study of their positions, through the 2D distribution function $h(x, y)$ that reflects the probability of finding an oxygen atom of water at position (x, y) whatever its z position. Such distribution functions $h(x, y)$ for 13 water molecules adsorbed on a hydroxylated surface containing one OH site are given in Figure 4. These functions give not only structural results, but they also contain indirect information on the mobility of the aggregate, because they are averaged over the whole simulation duration. On the hydroxylated surface at 100 K (Figure 4a), water molecules tend to remain bound to the OH site, as indicated by the density distribution around this site (high density in $h(x, y)$). On the contrary, water moves more freely at 250 K, as indicated by

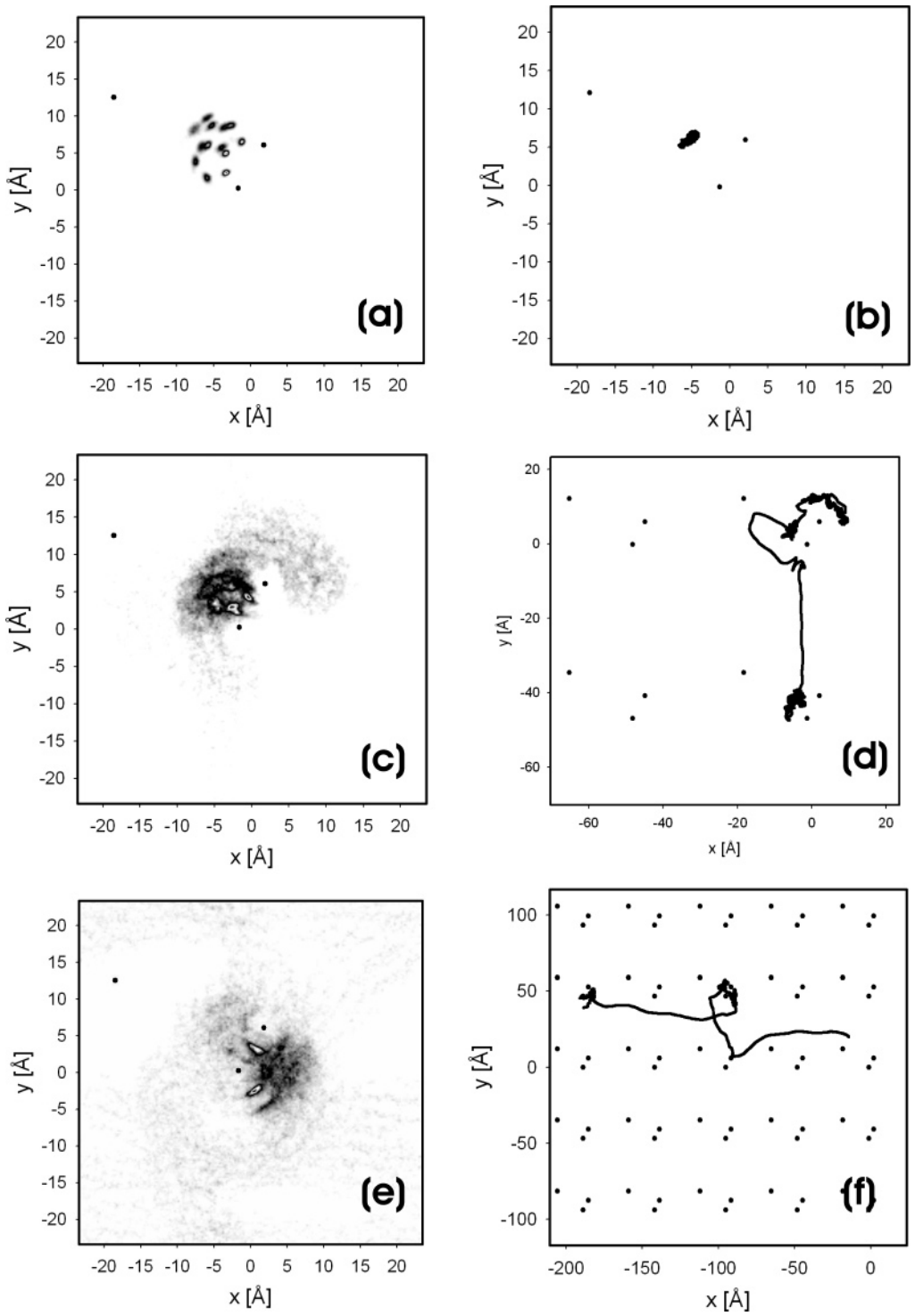

Figure 7. Same Plots as Figure 6, but for a random scattering where the three OH sites are close to each other on the hydroxylated surface (set 2).

the spreading of the corresponding distribution (Figure 4c). At 200 K, an intermediate behavior is evidenced with a distribution $h(x, y)$ which is less marked around the OH site than at 100 K (Figure 4b).

Finally, we have investigated the dynamics of the water aggregate above the hydroxylated surface (one OH site) by calculating the trajectories of the aggregate center of mass in the (x, y) plane of the surface, at different temperatures (Figure 5). At 100 K, the trajectory of the aggregate center of mass remains confined around the OH site, indicating that the water aggregate stays tied to the OH site during the whole simulation, at a distance of about 5 Å from the O atom of the OH site. In contrast, at 250 K, the mobility of the water aggregate appears sufficiently large to move over the whole MD box, with no significant permanent attachment to the OH site. At 200 K, an intermediate behavior is again evidenced for the water aggregate, which can move on the surface, with however some periods of significant attachment to the OH site.

Note that, in the simulations, due to periodic conditions, when the trajectory leaves the MD box from one side, its symmetric image enters the box from the other side. In Figure 5, we have chosen to represent the trajectory in a large system containing the simulation box itself and its periodic images, for clarity. As a consequence, the figure contains a juxtaposition of

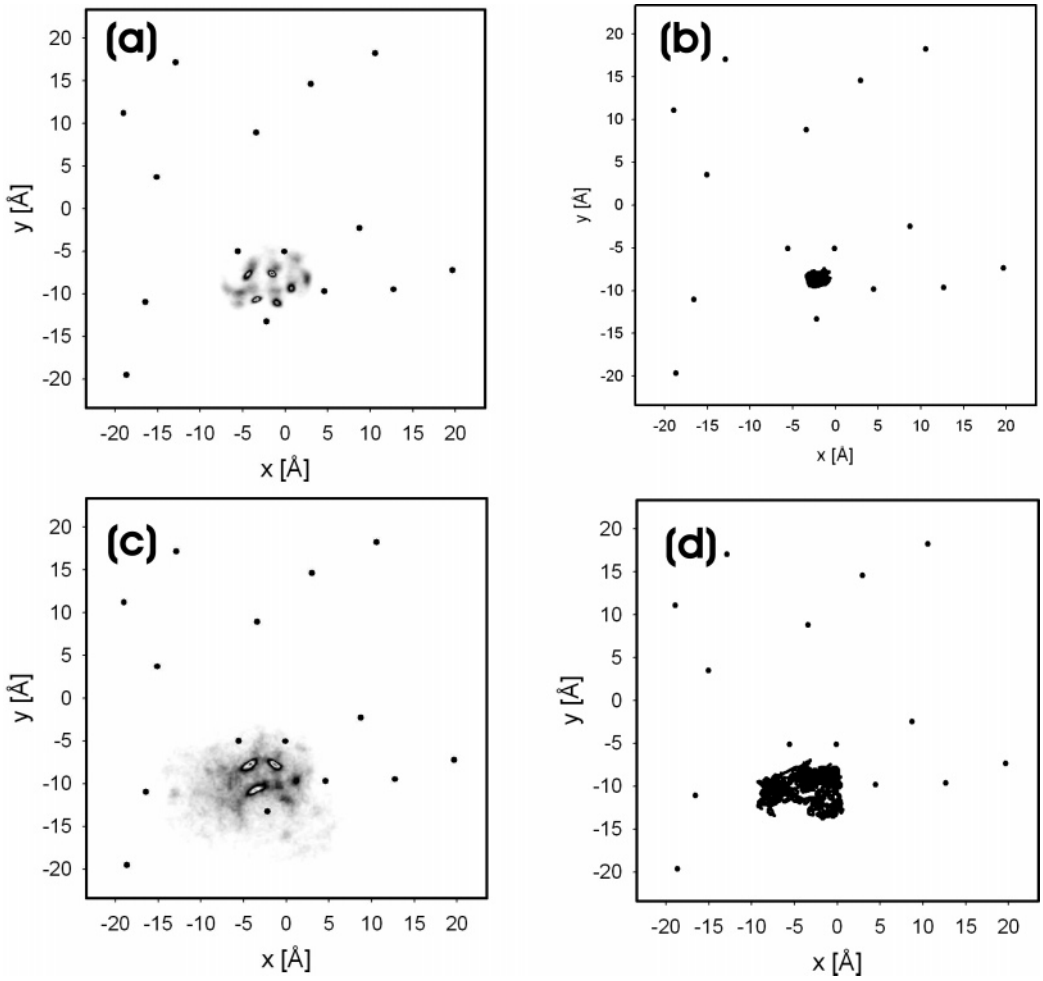

Figure 8. Distribution functions $h(x, y)$ of the oxygen atoms (of water molecules) positions projected in the (x, y) plane of the surface and trajectories of the aggregate center of mass for an aggregate containing 13 water molecules at 200 (a and c, respectively) and 250 K (b and d), above a surface containing 15 OH sites (black circles).

equivalent boxes, and then exhibits several OH sites (1 OH site per MD box). A careful time analysis of this trajectory shows however that, in the range of stratospheric temperatures, the displacements of the water aggregates is perturbed by the presence of the OH site, only if it moves close to this site with one water molecule in a configuration favorable to the formation of one hydrogen bond. There, the water aggregate spends some time around this OH site. In that way, the dynamical behavior of the water aggregate is different to that calculated on a bare graphite surface at the same temperatures (200 and 250 K, not shown), where there are no trapping sites.

To characterize more precisely the attachment of the water aggregate to the OH site, we have performed a statistical analysis of the time spent by the water molecules around this site. By considering that the aggregate is attached to the OH site as long as one O−H pair is closer than 2.5 Å (i.e., as long as one atom O (or H) pertaining to this aggregate is located at a distance less than 2.5 Å from one atom H (or O, respectively) of the OH site), the MD simulations at 100 K indicate that the water aggregate spends 83% of the simulation duration attached to the OH site, whereas this number decreases to 25% and 18% of the simulation duration at 200 and 250 K, respectively. This confirms that the mobility of the water aggregate is strongly hindered by the presence of the OH site on the graphite surface at very low temperature but is not significantly modified by this OH site at higher temperatures characteristic of the troposphere.

3.3. Simulations with Several Active Sites on the Graphite Surface. After investigating the behavior of a small water aggregate interacting with a hydroxylated graphite surface containing one OH site, we carried out simulations with a random distribution of OH sites on the graphite surface, to get information on the influence of such concentrations of hydroxyl sites on this water aggregate adsorption.

Let us illustrate these results by first considering a simulation box containing 13 water molecules adsorbed on a graphite surface containing three active sites, scattered in such a way that these sites are located quite far from each other (set 1). The corresponding adsorption energy is given in Table 4. It is largely dominated by the lateral interactions between water molecules that account for more than 85% of the total potential energy. These lateral interactions lead to the formation of a water aggregate whatever the temperature considered in the present study, as confirmed by the pair radial distribution functions $g_{O-cm}(r)$ (not shown) that indicate a limited spatial extension of the O atoms with respect to the center of mass of the 13 water molecules.

The distribution functions $h(x, y)$ corresponding to these 13 water molecules are given in Figure 6a (100 K), c (200 K), and e (250 K). These distributions show that the water molecules remain localized around one of the three OH sites at 100 K; that is, the water aggregate stays attached to the same OH site during the whole simulation. This is confirmed by the calculation of the trajectory in the (x, y) plane of the water aggregate center

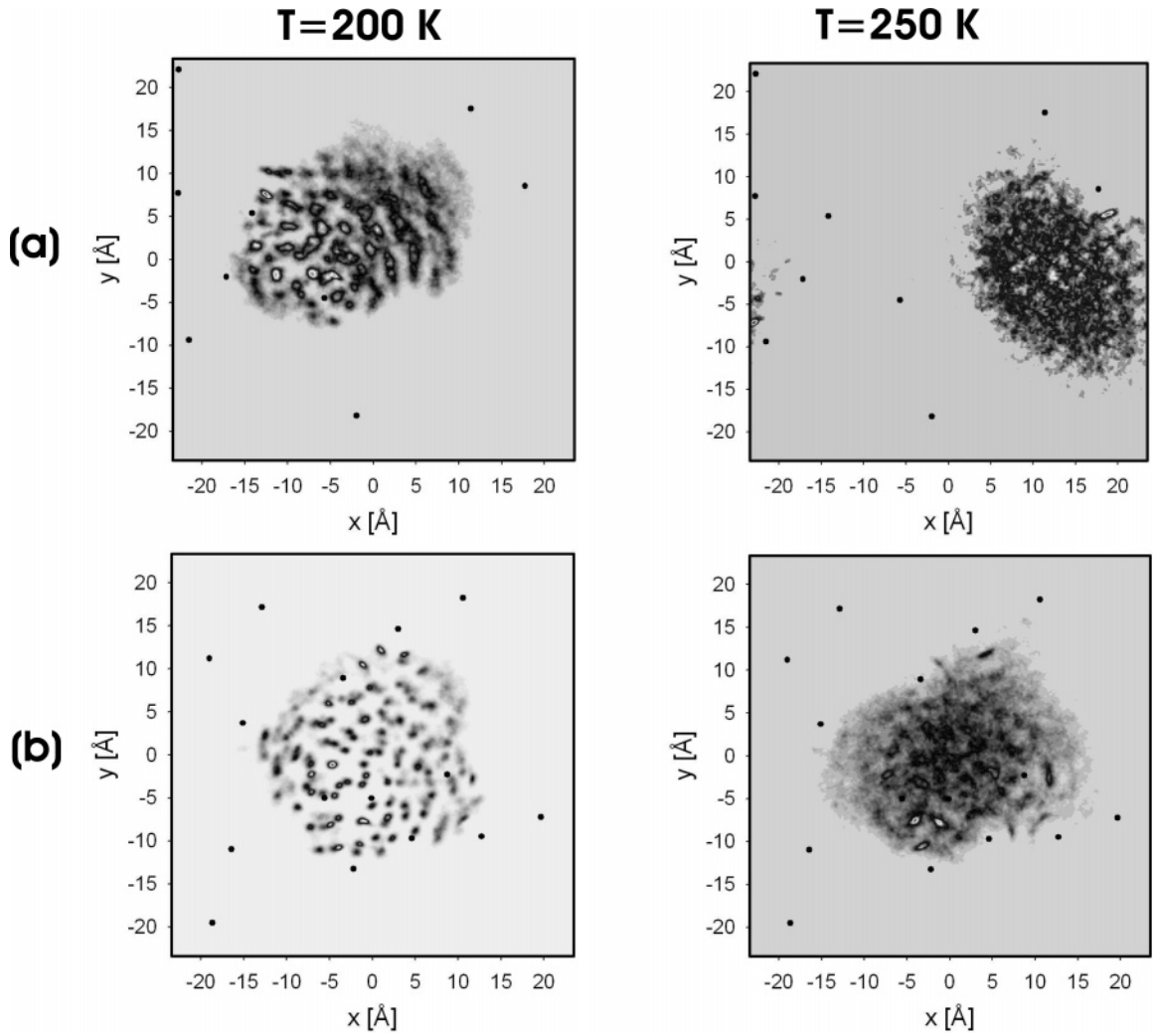

Figure 9. Distribution functions $h(x, y)$ of the positions of the oxygen atoms (of water molecules) projected in the (x, y) plane of the surface, for an aggregate containing 128 water molecules adsorbed on a surface containing (a) 9 and (b) 15 OH sites, at 200 (left-hand side) and 250 K (right-hand side).

of mass (Figure 6b) that evidences the localization of the aggregate around the same OH site. At 200 K, the water aggregate remains mainly attached to one of the three OH sites (Figure 6c), although it can explore the vicinity of a second OH site, as illustrated by its trajectory in the (x, y) plane (Figure 6d). In contrast, at 250 K, $h(x, y)$ exhibits dark gray zones around the three OH sites (Figure 6e), indicating that these three regions are explored by the water molecules during the simulations. However, because these water molecules form a stable aggregate during the whole simulation (as demonstrated by the analysis of $g_{O-cm}(r)$, not shown), $h(x, y)$ can be interpreted by considering that this single water aggregate explores successively the three OH regions during the simulation. This is confirmed by the representation of its trajectory on the hydroxylated graphite surface at 250 K (Figure 6f).

To characterize the influence of the OH sites scattering on the surface, we have also performed similar simulations by considering three OH sites randomly scattered in such a way that they are localized in the same region of the surface (set 2). The corresponding results are given in Table 4 and Figure 7. From an energetic point of view, the results are very similar to that obtained with the previous distribution of OH sites, with however a slightly more important contribution of the water−surface interactions. In the same way, the analysis of $g_{O-cm}(r)$ (not shown) also indicates the formation of a stable water aggregate at 100, 200, and 250 K. This aggregate remains strongly localized in the vicinity of the two nearest OH sites at 100 K (Figure 7a and b), that act as a strong "double site" trapping for the water molecules. The main difference with the previous distribution of OH sites on the graphite surface (set 1) is observed at higher temperature (200 and 250 K). Indeed, the dark gray zone in Figure 7c and e, together with the analysis of the trajectory of the water aggregate (Figure 7d and f), indicates that the water molecules explore mainly the region located around the double site, with no durable attachment on the third (isolated) OH site.

Finally, we have performed simulations with a very high density of OH sites on the graphite surface (namely 15 sites), at 100, 200, and 250 K. For these temperatures, the water molecules form again an aggregate, that behaves as a whole entity on the hydroxylated surface. However, in contrast to the situations detailed above, such a high density of OH sites on the surface leads to a strong localization of the water aggregate for all temperatures considered, as indicated by the distribution functions $h(x, y)$ and the trajectories given in Figure 8 (note that the results at 100 K are not shown because they are very similar to those obtained at 200 K). In fact, the water aggregate remains confined during the whole simulation in a region of the hydroxylated surface where the density of OH sites is high. Note that we have checked that different initial positions for the water aggregate always leads to the same confinement in the vicinity of close OH sites. As a consequence of both the

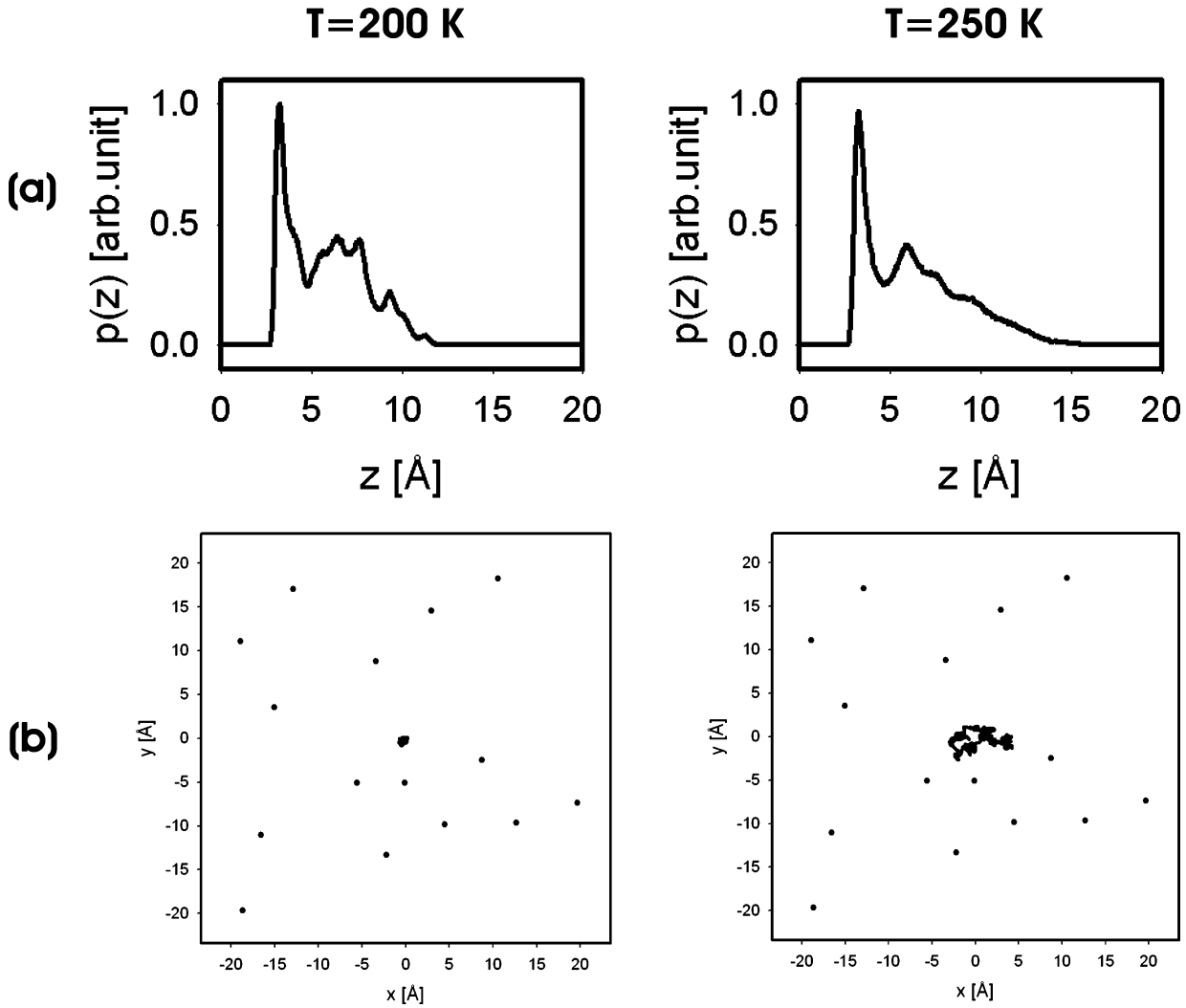

Figure 10. (a) Distribution functions $p(z)$ of the z position perpendicular to the graphite plane of the oxygen atoms (of water molecules) and (b) trajectories of the aggregate center of mass for an aggregate of 128 water molecules adsorbed on a hydroxylated graphite surface containing 15 OH sites, at 200 (left-hand side) and 250 K (right-hand side).

high density of OH sites on the surface and the confinement of the water molecules around these sites, the contribution of the molecule−surface interactions is higher than in the situations studied above and accounts for about 20% of the total interactions (Table 4).

To summarize, the present study of a few water molecules adsorbed on a hydroxylated graphite surface shows that the behavior of these water molecules is mainly driven by the density and the localization of the OH sites, rather than by the water−surface interactions.

3.4. Simulations with Several Active Sites on the Graphite Surface and Larger Water Coverages. After investigating the behavior of a small amount of water molecules on different hydroxylated graphite surfaces, we performed simulations with higher water coverage (namely, 39, 48, and 128 water molecules) on the same hydroxylated graphite surfaces.

The corresponding adsorption energies are given in Table 4 and show again that the lateral interactions V_{ww} between water molecules largely dominate the total adsorption energy whatever the hydroxylated graphite surface, with a contribution of V_{ww} that increases from about 90% to about 95% when the number of water molecules increases from 39 to 128.

The distribution functions $h(x, y)$ corresponding to the largest amount of water molecules considered in the present simulations (128 molecules) are given in Figure 9 for two different surfaces containing 9 and 15 randomly scattered OH sites. This figure shows that the water molecules remain clustered together at 100, 200, and 250 K, whatever the density of OH sites on the surface and that they form a large aggregate on the surface. This conclusion is also supported by the analysis of the distribution function $p(z)$ of the water molecule centers of mass along the z direction perpendicular to the graphite surface that is characterized by several peaks indicating a three-dimensional arrangement of the water molecules (Figure 10a). This is also confirmed by calculation of the pair radial distribution functions $g_{O-cm}(r)$ (not given) that show a spatially limited extension of the O atoms distribution around the center of mass of the water molecules. Indeed, the spatial extension of the water molecules around the center of mass of the corresponding aggregate is limited to about 10 Å for the three temperatures considered in the present simulations.

Clearly, the interaction with the hydroxylated graphite surface is too weak to counterbalance the large water−water interactions at high coverage. As a consequence, water molecules form a stable 3D aggregate rather than an "as stretched as possible" aggregate, as obtained previously on a graphite surface containing COOH sites.[15] However, this aggregate remains confined in the vicinity of the surface region characterized by the highest density of OH sites, as indicated by the analysis of its trajectories at 200 and 250 K (Figure 10b). Very similar features are

obtained when considering 39 and 48 water molecules in the simulations and lower temperature (100 K).

4. Conclusion

In the present paper, we characterize the interaction between water molecules and hydroxylated graphite surfaces by modeling typical surfaces of soot particles. This work is a natural continuation of our previous works devoted to the interaction between partially oxidized graphite surfaces and water.[14−17] The results of molecular dynamics simulations performed at temperatures typical of the boundaries of the tropospheric temperature range (200 and 250 K), and at a much lower temperature (100 K) for comparison, show that the water−OH sites interaction is quite weak compared to the water−water interaction. This leads to the clustering of the water molecules above the surface, and the corresponding water aggregate can only be trapped by the OH sites at low temperature (100 K, and to a lesser extent 200 K), or when the density of OH sites is sufficiently high. Moreover, the present results show that the behavior of water molecules interacting with hydroxylated graphite surfaces is mainly driven by the density and the localization of the OH sites, rather than by the water−surface interactions. In addition, no significant difference has been evidenced in the dynamical behavior of the water aggregates within the tropospheric temperature range.

The results obtained in the present study at 250 K differ from those obtained at the same temperature when considering COOH sites on the graphite surface instead of OH sites.[15] Indeed, our previous studies show that the interactions between COOH and the water molecules are much stronger than those between OH and water[16,17] and that the COOH sites act as strong trapping sites for the first adsorbed water molecules that then become nucleation centers for larger water aggregates tied to the COOH sites. This strong trapping is a consequence of the possible formation of two H-bonds between the COOH site and the water aggregate. On a surface containing a high density of COOH sites, this also leads to the formation of a as stretched as possible water aggregate.[15] On the contrary, on a hydroxylated graphite surface, the present simulations clearly show that the interaction with one OH site is not strong enough to trap the water molecules in the stratospheric range of temperatures between between 200 and 250 K. The water molecules rather form a 3D aggregate moving more or less freely above the surface. Such a trapping is only observed when considering a small amount of water molecules, when the temperature is sufficiently low to hinder the dynamics of the water aggregate, and/or when the number of OH sites on the surface is sufficiently high to compete with the lateral interactions between water molecules and to confine the water aggregate between neighboring OH sites.

Finally, it is important to note that such a difference between partially oxidized graphite surfaces should be taken into account in the interpretation of experimental results. For example, in an experimental study of the water adsorption on oxidized carbon surfaces, it has been inferred a few years ago that the water−oxide interaction is essentially independent of the actual structure (phenolic, carboxylic, carbonylic, ...) in which the oxygen atom is incorporated.[28] Such a conclusion should certainly be reconsidered on the basis of the present results.

Acknowledgment. This work was supported by the "Agence de l'Environnement et de la Maîtrise de l'Energie (ADEME)" through the PRIMEQUAL2-PREDIT program (No. 04 06 C0047).

References and Notes

(1) Popovicheva, O. B.; Persiantseva, N. M.; Trukhin, M. E.; Rulev, G. B.; Shonija, N. K.; Buriko, Y. Y.; Starik, A. M.; Demirdjian, B.; Ferry, D.; Suzanne, J. *Phys. Chem. Chem. Phys.* **2000**, *2*, 4421.

(2) Popovicheva, O. B.; Persiantseva, N. M.; Kuznetsov, B. V.; Rakhmanova, N. K.; Shonija, N. K.; Suzanne, J.; Ferry, D. *J. Phys. Chem. A* **2003**, *107*, 10046.

(3) Popovicheva, O. B.; Trukhin, M. E.; Persiantseva, N. M.; Shonija, N. K. *Atmos. Environ.* **2001**, *35*, 1673.

(4) Chen, Y.; Kreidenweiss, S. M.; McInnes, L. M.; Rogers, D. C.; DeMott, P. J. *Geophys. Res. Lett.* **1998**, *25*, 1391.

(5) DeMott, P. J.; Chen, Y.; Kreidenweiss, S. M.; McInnes, L. M.; Rogers, D. C.; Sherman, D. E. *Geophys. Res. Lett.* **1999**, *26*, 2492.

(6) Seinfeld, J. H. *Nature* **1998**, *391*, 837.

(7) Aksenenko, E. V.; Tarasevich, Y. I. *Adsorp. Sci. Technol.* **1996**, *14*, 383.

(8) Tarasevich, Y. I.; Zhukova, A. I.; Aksenenko, E. V.; Bondarenko, S. V. *Adsorp. Sci. Technol.* **1997**, *15*, 497.

(9) Tarasevich, Y. I.; Aksenenko, E. V. *Colloids Surf., A* **2003**, *215*, 285.

(10) Müller, E. A.; Rull, L. F.; Vega, L. F.; Gubbins, K. E. *J. Phys. Chem.* **1996**, *100*, 1189.

(11) Müller, E. A.; Gubbins, K. E. *Carbon* **1998**, *36*, 1433.

(12) McCallum, C. L.; Bandosz, T. J.; McGrother, S. C.; Müller, E. A.; Gubbins, K. E. *Langmuir* **1999**, *15*, 533.

(13) Jorge, M.; Schumacher, C.; Seaton, N. A. *Langmuir* **2002**, *18*, 9296.

(14) Hamad, S.; Mejias, J. A.; Lago, S.; Picaud, S.; Hoang, P. N. M. *J. Phys. Chem. B* **2004**, *108*, 5405.

(15) Picaud, S.; Hoang, P. N. M.; Hamad, S.; Mejias, J. A.; Lago, S. *J. Phys. Chem. B* **2004**, *108*, 5410.

(16) Collignon, B.; Hoang, P. N. M.; Picaud, S.; Rayez, J. C.; *Chem. Phys. Lett.* **2005**, *406*, 431.

(17) Collignon, B.; Hoang, P. N. M.; Picaud, S.; Rayez, J. C.; *Comput. Lett.* **2005**, *1*, 277.

(18) Allen, M. P.; Tildesley, D. J. In *Computer Simulations of Liquids*; Clarendon: Oxford, UK, 1987.

(19) Shevade, A. V.; Jiang, S.; Gubbins, K. E. *J. Chem. Phys.* **2000**, *113*, 6933.

(20) Jorgensen, W. L.; Madura, J. D. *J. Am. Chem. Soc.* **1983**, *105*, 1407.

(21) Singh, U. C.; Kollman, P. A. *J. Comput. Chem.* **1984**, *5*, 129.

(22) Besler, B. H.; Merz, K. M., Jr.; Kollman, J. P. A. *J. Comput. Chem.* **1990**, *11*, 431.

(23) Mahoney, M. W.; Jorgensen, W. L. *J. Chem. Phys.* **2000**, *112*, 8910.

(24) Jorgensen, W. L.; Chandrasekhar, J.; Madura, J. F.; Impey, R. W.; Klein, M. L. *J. Chem. Phys.* **1983**, *79*, 926.

(25) Spohr, E. *J. Chem. Phys.* **1997**, *107*, 6342.

(26) Lisal, M.; Kolafa, J.; Nezbeda, I. *J. Chem. Phys.* **2002**, *117*, 8892.

(27) Eisenberg, D.; Kauzmann, W. In *The Structure and Properties of Water*; Clarendon: Oxford, UK, 1969.

(28) Barton, S. S.; Evans, M. J. B.; MacDonald, J. A. F. *Langmuir* **1994**, *10*, 4250.